Original article
DOI: https://doi.org/10.18721/JPM.14406

DEVELOPMENT OF THE PORTABLE COLD PLASMA SOURCE FOR BIOMEDICAL APPLICATIONS

E. G. Feklistov ✉

Peter the Great St. Petersburg Polytechnic University, St. Petersburg, Russia

✉ efrem.feklistov@mail.ru

Abstract: A cold plasma source (CPS) developed by us has been put forward. The operating principle of the device is based on the use of a pulsed positive corona discharge at atmospheric pressure. The CPS exhibits compactness and autonomy. Particularly, the weight of the handheld plasma source is 80 g with the mass of the portable battery pack not exceeding 100 g. The electrical characteristics of electrode systems designed for direct and indirect treatment of biomedical objects with cold plasma were investigated. It was shown that in the studied electrode gaps the discharge exists in a streamer mode characterized by repetitive nanosecond current pulses in the range of 10 – 80 mA at operating voltages up to 10 kV. It was found that for the electrode system developed for indirect generation of cold plasma, the voltage range corresponding to stable discharge is wider than that for the system designed for the direct one.

Keywords: cold plasma source, corona discharge, streamer discharge, electrode systems, biomedicine

Financing: the work was done with financial support of the Russian Foundation for Basic Research within the framework of a science project, grant No. 20-38-90161.

Citation: Feklistov E. G., Development of the portable cold plasma source for biomedical applications, St. Petersburg Polytechnical State University Journal. Physics and Mathematics. 14 (4) (2021) 84–94. DOI: 10.18721/JPM.14406

Научная статья
УДК 537.523.3
DOI: https://doi.org/10.18721/JPM.14406

РАЗРАБОТКА ПОРТАТИВНОГО ИСТОЧНИКА ХОЛОДНОЙ ПЛАЗМЫ ДЛЯ БИОМЕДИЦИНСКИХ ПРИЛОЖЕНИЙ

Е. Г. Феклистов✉

Санкт-Петербургский политехнический университет Петра Великого, Санкт-Петербург, Россия

✉ efrem.feklistov@mail.ru

Аннотация. Предлагается разработанный источник холодной плазмы, принцип работы которого основан на использовании импульсного положительного коронного разряда атмосферного давления. Устройство обладает компактностью и автономностью, вес ручного плазменного источника составляет 80 г при массе выносного блока питания, не превышающей 100 г. Исследованы электрические характеристики электродных систем, предназначенных для прямой и косвенной обработки биомедицинских объектов холодной плазмой. Показано, что в исследуемых электродных промежутках разряд существует в стримерной форме, характеризующейся наносекундными периодическими импульсами тока в диапазоне 80 – 10 мА при напряжениях до 10 кВ. Установлено, что для электродной системы с косвенной генерацией холодной плазмы диапазон напряжений, соответствующий стабильному горению разряда, шире, чем для системы с прямой генерацией.

Ключевые слова: источник холодной плазмы, коронный разряд, стримерный разряд, электродные системы, биомедицина

Финансирование: Исследование выполнено при финансовой поддержке РФФИ в рамках научного проекта № 90161-38-20.

Ссылка при цитировании: Феклистов Е.Г. Разработка портативного источника холодной плазмы для биомедицинских приложений // Научно-технические ведомости СПбГПУ. Физико-математические науки. 2021. Т. 14. № 4. С. 84–94. DOI: 10.18721/JPM.14406

Introduction

Gas discharge physics is a burgeoning field of science and technology. The last decades have seen unprecedented interest towards this area as gas-discharge sources find novel applications in plasma medicine [1]. In this case, the gas discharge serves as a source of cold plasma where the temperature of ions and neutral particles does not exceed several tens of degrees Celsius [2]. Ultraviolet radiation, electric fields, reactive species, and electric currents are generally considered as the main phenomena underlying the operation of plasma sources [3]. As a matter of fact, the evolution of gas-discharge processes results in producing radicals, excited particles and ions, primarily through electron-molecule and ion-molecule collisions. These particles are generated within the first hundreds of nanoseconds, which corresponds to the time it takes for streamer discharge to develop [4].

The most peculiar chemical species with a biological effect include superoxide oxygen radical ($\cdot O_2^-$), ozone (O_3), hydroxyl radical ($\cdot OH$), hydrogen peroxide (H_2O_2), peroxyl radical ($HO_2\cdot$), nitrogen monoxide (NO) and peroxonitric acid (HNO_4) [5].

The non-equilibrium of cold plasma, combining a high level of electron energy and a high concentration of reactive species at a low gas temperature allows using it in biology and medicine. Current applications of cold plasma include sterilization of surfaces, inactivation of pathogenic microorganisms, disinfection of gas and liquid media, food processing, cell stimulation and wound healing [6].

Therefore, constructing electrophysical devices for generating cold plasma (cold plasma sources) is of crucial importance, laying the groundwork for future research and technologies in engineering sciences and biomedicine.

Glow, dielectric-barrier, corona and high-frequency discharges can serve as cold plasma sources [1, 2]. Cold plasma is generated in this study by a corona discharge (CD) at atmospheric pressure. The corona type of gas discharge was specifically chosen to produce reactive species, transferring them to the object treated through electrohydrodynamic flows [7]. What is more, this type of discharge can reduce the risk of electric shock compared to, for example, barrier discharge. The electrode gap in the CD can be divided into two regions: ionization (corona sheath) and drift [8]. The first one extends a very short distance from the discharge electrode and is characterized by an electric field with a high strength. The second one, the drift region, makes up the rest of the electrode gap.

CD has been well-established to be an extremely undesirable effect in the electric power industry due to the resulting power losses and radio frequency interference. At the same time, CD is widely used in surface treatment of materials [9], in electrostatic precipitators and in ozone production [10]. Furthermore, CD has found biomedical applications due to its newly discovered bactericidal effect [11, 12]. The polarity of the corona electrode apparently has a strong effect on gas discharge processes. For example, negative CD is characterized by

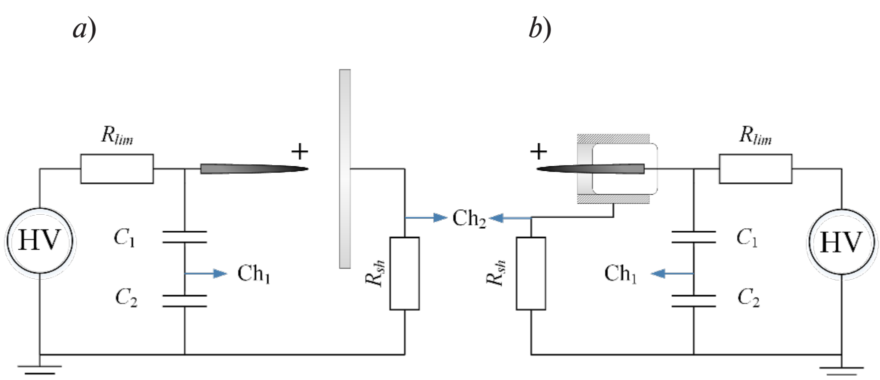

Fig. 1. Schematic of experimental setup for direct (*a*) and indirect (*b*) CD generation: Ch_1, Ch_2 are the channels of the digital oscilloscope recording voltage and current, respectively; HV are high-voltage sources; C_1, C_2 are the capacitances of voltage dividers; R_{lim} are the current-limiting resistances; R_{sh} are the current shunts

Trichel pulses with amplitudes of the order of 2–10 mA and frequencies of about 10^5 Hz [8, 13]. A positive CD successively passes from diffuse to streamer mode with increasing voltage, ultimately turning to spark. Ozone dominates among reactive oxygen species in the case of negative CD [14], while superoxide anions O_2^- are the main charge carriers reaching the anode. Positive CDs typically generate less ozone in the air than negative CDs at the same voltage level. If CD is generated in a closed space, the accumulated chemical species affect the electrical characteristics of the discharge [15]. Two main CD systems are commonly used in biological experiments, involving direct and indirect schemes for plasma generation. Biological samples are positioned between the discharge and ground electrodes in the direct scheme; the sample can be placed behind the ground electrode made as a mesh in this case in the indirect scheme. The advantage of the indirect treatment over the direct method is that the samples are strongly exposed to reactive species generated by the CD at a minimum level of discharge current.

The goal of this study consisted in developing a cold plasma source using a positive corona discharge at atmospheric pressure.

We intended to explore the discharge characteristics in different electrode systems of the cold plasma source at atmospheric pressure for biomedical applications.

Experimental methods

We considered the gas-discharge characteristics for direct and indirect schemes of cold plasma generation. Stainless steel needles with a curvature radius of about 40 μm were used as a discharge electrode. A simplified schematic of the experimental setup is shown in Fig. 1. A high positive potential was applied to the needle through a current-limiting resistance R_{lim} = 10–30 MΩ from a MANTIGORA HT-2000P constant voltage source. The cathode was shaped as a flat disk in the direct scheme (Fig. 1,*a*). The scheme with indirect CD generation in our experiments differs from that described in Introduction: the cathode is shaped as a cylindrical electrode (Fig. 1, *b*). The high potential was separated from the zero potential with a cylindrical plate made of polytetrafluoroethylene in this system. A LeCroy WaveJet 2Gs/s two-channel oscilloscope was used to record the rapidly varying characteristics. The discharge current was measured with a low-inductive resistor R_{sh} with a resistance of 43 Ohm, while the voltage across the gas discharge gap was measured using a high-voltage capacitive divider (division ratio of 1:1000). The capacitance C_1 in the upper arm was approximately 0.1 pF, making it possible to reduce the influence of the measurement circuit on the gas-discharge process.

Corona discharge generation schemes

The electrical circuit of the cold plasma source should ensure stable operation of the generator for both direct and indirect treatment schemes. The diagram in Fig. 1,*a* corresponds to direct generation of cold plasma, since the sample treated is galvanically (directly) coupled to the electrode system of the generator via the ground electrode in this case. It is then evident that most of the current flow lines form closed loops in the given sample. On the other hand, most of the current flow lines in the case of indirect CD generation form closed loops in the electrode with zero potential (Fig. 1,*b*), while the sample treated is galvanically isolated from the generator electrode system. Both schemes have their advantages and disadvantages. Direct plasma generation allows treating the surface not only by ions and reactive species but also through direct exposure to discharge streamers, which can be useful for sterilizing surfaces. However, this can destroy cell cultures and some types of tissues (for example, the epithelium of mucous membranes). Indirect plasma generation minimizes the effect of discharge current. Even though most of the electric current lines cross the treated sample, reactive species and ions are carried to its surface due to ionic wind.

Results and discussion

Cold plasma parameters. Corona discharge exists in streamer mode in the cold plasma sources under consideration. The densities of electrons and ions reach values around 10^{13}–10^{14} cm^{-3} at the tip of the corona needle and in the streamer head [16]. In this case, the degree of ionization is approximately 10^{-6}–10^{-5}. The positive CD plasma is predominantly composed of N_2^+, N_4^+, O_2^+, H_2O^+, O_2^-, OH^-, H^- ions produced through the following reactions [17, 18]:

$$
\begin{gathered}
N_2 + e^- = N_2^+ + 2e^- \, (15.60 \text{ eV}), \\
O_2 + e^- = O_2^+ + 2e^- \, (12.06 \text{ eV}), \\
N_2^+ + N_2 + M = N_4^+ + M \, (5 \cdot 10^{-29} \text{ cm}^6 \text{s}^{-1}), \\
H_2O + e^- = H_2O^+ + 2e^- \, (13.00 \text{ eV}), \\
O_2 + e^- + M = O_2^- + M \, (\sim 10^{-30} \text{ cm}^6 \text{s}^{-1}), \\
H_2O + e^- = OH^- + H \, (3.58 \text{ eV}), \\
H_2O + e^- = H^- + OH \, (4.36 \text{ eV}), \\
H_2O + e^- = H_2 + O^- \, (3.28 \text{ eV})
\end{gathered}
\tag{1}
$$

(either the ionization energies (eV) or the reaction rate constants ($cm^6 \cdot s^{-1}$) are given in parentheses).

Notably, the densities of negative ions and H_2O^+ ions strongly depend on the pressure of water vapor in the air [8].

In addition to ionized species, the generated plasma also contains excited particles. Bands of the N_2 second positive system with a dominant peak at 337.1 nm are clearly detectable in the wavelength range of 300–400 nm. This system is connected with the vibrational levels of the nitrogen molecule [19]. The time-averaged conductivity of the gas-discharge gap is about 0.001–0.1 S/m.

Pulses of CD currents and voltages. Given high values of the product *pd* (*p* is the pressure, *d* is the distance between the electrodes) and the potentials exceeding the CD ignition voltage, the positive corona discharge exists in streamer form. In this case, the streamer begins near a point corresponding to a region with a higher electric field, favoring intense electron multiplication. Even though a constant voltage is applied to the gas-discharge gap through the limiting resistance, the potential across the needle bears a repetitively pulsed character (Fig. 2).

The voltage across the air gap varies periodically on a microsecond scale between the magnitude of discharge ignition and extinction by the law

$$u(t) = U_0 + (U_{ex} - U_0)\exp(-t/\tau), \tag{2}$$

while the voltage at the end of the air gap charging period is

$$u(T) = U_{ig}, \tag{3}$$

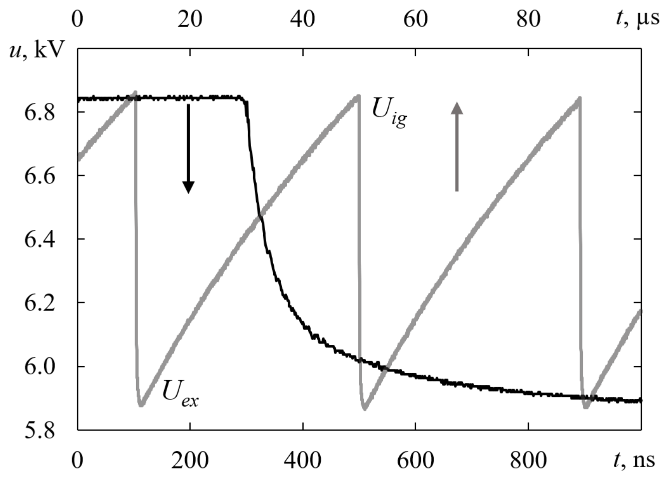

Fig. 2. Waveforms of the potential across the needle tip.
The ignition (U_{ig}) and extinction (U_{ex}) potentials are shown on voltage pulses;
the arrows indicate timescale counts

where U_{ig}, U_{ex}, V, are the levels of ignition and extinction, respectively; U_0, V, is the source voltage; t, s, is the time; T, s, is the pulse repetition period; τ, s, is the time constant of the charging process whose magnitude depends on the total capacitance of the discharge system and the magnitude of the limiting resistance.

The discharge mode considered can be characterized by two time scales, nano- and microsecond. The small scale corresponds to streamer processes, and the large scale corresponds to space charge relaxation and voltage recovery to the ignition level U_{ig}. The pulse repetition rate depends on the source potential, the equivalent capacitance, and the parameters of the electrode gap. In addition, the above processes evolve stochastically, resulting in a certain spread in frequency.

Fig. 3 shows the waveforms of current and voltage pulses on a nanosecond scale for the needle-plane system. Evidently, the amplitude of the current pulses decreases with an increase in the gas-discharge gap. The difference between the ignition (U_{ig}) and extinction (U_{ex}) voltages increases. The leading edge of the current pulses corresponds to the stage when a streamer directed towards the cathode forms and propagates (10–30 ns). A sharp increase in the corona current before the first peak corresponds to the contact between the streamer head and the cathode. After the streamer arrives at the cathode from the anode, a secondary streamer evolves, which can be reflected by the second pulse peak in the current waveforms (d = 8 and 10 mm). Relaxation of the discharge current is observed next for a time period of about 300 ns. The process subsequently resumes as soon as the voltage across the air gap reaches the ignition level. The behaviors observed for the needle-cylinder system are the same as described above, but the amplitudes of the current pulses are lower by about 20–30%.

Current-voltage characteristics of CD. The experiments carried out have established that the average current increases quadratically with an increase in the applied voltage (Fig. 4), which is typical for CD. This increase is due to the space charge effect. There are two well-known formulations of the law describing the current-voltage characteristics of CD: Townsend's formula and a simplified version of Henson's formula [20, 21].

We preferred to use the Townsend formula to approximate the experimental data for the purposes of this study:

$$I = AU(U - U_{in}), \tag{4}$$

where A is a constant coefficient accounting for the contributions from the geometry of the electrode system, the effective mobility of charge carriers and the relative permittivity of the medium; U_{in} is the initial voltage of the CD.

The law describing the rise in the average current deviates from quadratic dependence given a substantial increase in voltage, which is due to stronger influence of streamer processes in this voltage range. The corresponding points did not fall into the approximated data sample. The

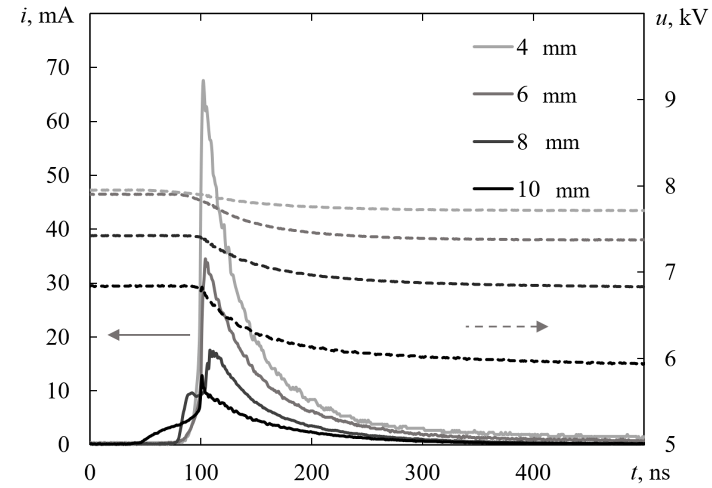

Fig. 3. Waveforms of current (solid lines) and voltage (dashed lines) pulses on the nanosecond scale for different distances d in the needle-plane system

a)

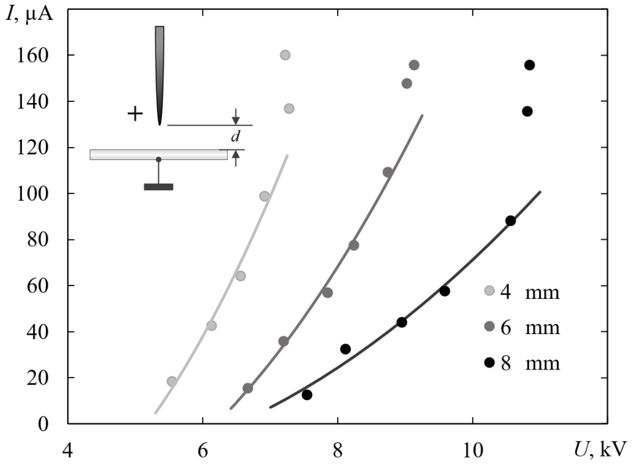

b)

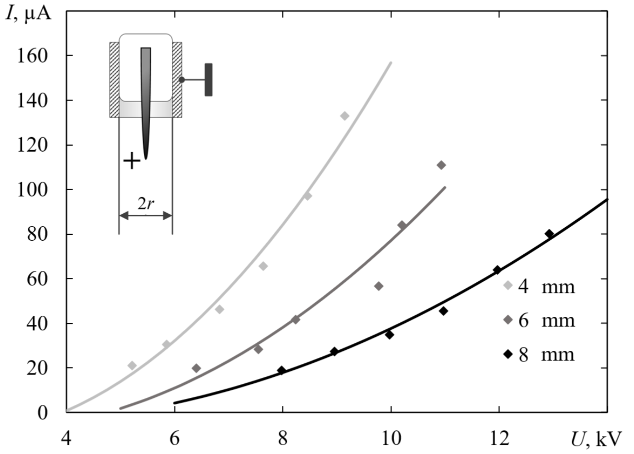

Fig. 4. Current-voltage characteristics of needle-plane (*a*) and needle-cylinder (*b*) systems for different electrode gaps *d* (*a*) and *r* (*b*)

quality of the approximation performed was characterized by a high value of the determination coefficient, $R^2 \geq 0.95$. Fig. 4,*a* shows the current-voltage characteristics for the needle-plane system. Evidently, the current rise rate increases with increasing electrode gap. The voltage at which CD begins increases from 5.2 to 6.5 kV when *d* changes from 4 to 8 mm.

Fig. 4,*b* shows the experimental current-voltage characteristics for the needle-cylinder system. Apparently, the average currents for the corresponding voltages and distances are lower here than those in the needle-plane system. However, the range of stable CD generation is wider in this case. The voltage at which the CD initiates increases from 3.9 to 5.1 kV when the electrode gap *r* (the radius of the hollow electrode) widens from 4 to 8 mm.

Cold plasma source. Fig. 5 shows the external view of the cold plasma source that we have constructed, with different types of electrode systems. The device can operate in both direct and indirect plasma generation modes depending on the electrode system used.

The source generating cold plasma includes several main units, enclosed in housing *1*: self-contained power source (*2* in Fig. 5,*a*); transistor switch; specially designed step-up transformer; high-voltage multiplier. The supply voltage is fed to the transistor from the self-contained source during operation, providing resonant generation of voltage pulses with an amplitude of 120–150 V and a frequency of 3–5 kHz.

The voltage is then increased by the transformer to 1.3–1.5 kV. After that, it is again increased to the required level (10–12 kV) by a high-voltage multiplier. Although the generator we constructed includes no system for forced air circulation, the reactive species reach the surface of

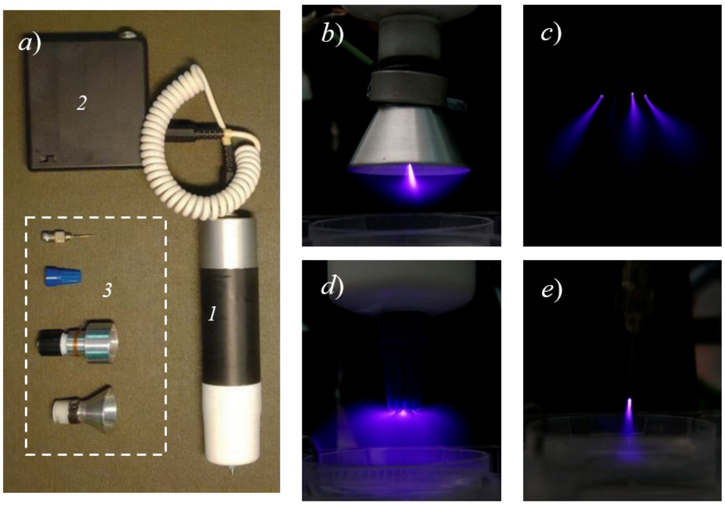

Fig. 5. Photo of portable cold plasma source *1* with self-contained power source *2* and different electrode systems (ES) *3* (*a*).
The following ES are shown: cone-shaped system for indirect generation of corona discharge (*b*), four-needle system with a dielectric casing (*d*) and without it (*c*), and single-needle system for direct generation of corona discharge (*e*)

the target treated due to ionic wind. Furthermore, the damaging effect from electric current is reduced in the case of CD compared with barrier discharge, where high power is required to ignite and maintain the discharge.

The electrical circuit of the constructed generator allows maintaining a stable gas discharge. The proposed cold plasma source *1* (see Fig. 5,*a*) has the following weight and dimensions: the outer diameter of the cylindrical housing is 28 mm, the length is about 150 mm with a total mass of 80 g. The self-contained power source *2* has the dimensions of 5 Ч 5 Ч 1 cm and weighs about 90 g. Single- and multi-needle systems are used as replaceable electrodes (see Fig. 5). The output ‘signal’ for the needle-plane system (d = 6–9 mm) has the following parameters. The discharge current amplitudes are in the range from 10 to 80 mA with a pulse repetition rate from 10 to 50 kHz. Moreover, the average discharge current is about 100 μA, so the risk of electric shock is eliminated for the cold plasma source constructed.

Conclusion

Comprehensive analysis of the latest advances in gas discharge physics carried out in this study was followed by construction of a cold plasma source. The device operates based on a pulsed positive corona discharge at atmospheric pressure. The source is compact and portable: the total weight of the source and the autonomous power supply unit does not exceed 170 g. We have obtained the electrical characteristics of electrode systems intended for direct and indirect treatment with cold plasma. We have established that the streamer mode of a corona discharge is generated in the given electrode gaps. The amplitudes of the current pulses do not exceed 100 mA at voltages up to 10 kV applied to the gap. The average corona discharge current increases quadratically in the voltage range from 5 to 15 kV. The streamer corona discharge transforms into spark discharge at high voltages. The voltage range corresponding to stable discharge is wider for an electrode system with indirect generation than for that with direct generation.

REFERENCES

1. **Fridman A., Friedman G.,** Plasma medicine, John Wiley & Sons Limited, Chichester, UK, 2013.
2. **Kong M. G., Kroesen G., Morfill G., et al.,** Plasma medicine: an introductory review, New J. Phys. 11 (11) (2009) 115012.
3. **Dobrynin D., Fridman G., Friedman G., Fridman A.,** Physical and biological mechanisms of direct plasma interaction with living tissue, New J. Phys. 11 (11) (2009) 115020.

4. **Dubois D., Merbahi N., Eichwald O., et al.,** Electrical analysis of positive corona discharge in air and N_2, O_2, and CO_2 mixtures, J. Appl. Phys. 101 (5) (2007) 053304.

5. **Sekimoto K., Gonda R., Takayama M.,** Effects of H_3O^+, OH^-, O_2^-, NO_x^- and NO_x for *Escherichia coli* inactivation in atmospheric pressure DC corona discharges, J. Phys. D. Appl. Phys. 48 (30) (2015) 305401.

6. **Weltmann K. D., von Woedtke T.,** Plasma medicine – current state of research and medical application, Plasma Phys. Control. Fusion. 59 (1) (2016) 014031.

7. **Moreau E., Audier P., Benard N.,** Ionic wind produced by positive and negative corona discharges in air, J. Electrost. 93 (June) (2018) 85¬96.

8. **Raizer Yu. P.,** Gas discharge physics., Springer, Berlin, New York, 1997.

9. **Castle G. P., Inculet I. I., Burgess K. I.,** Ozone generation in positive corona electrostatic precipitators, IEEE Trans. Industr. Gen. Appl. IGA-5 (4) (1969) 489–496.

10. **Giacometti J. A., Oliveira O. N.,** Corona charging of polymers, IEEE Trans. Electr. Insul. 27 (5) (1992) 924–943.

11. **Sysolyatina E., Mukhachev A., Yurova M., et al.,** Role of the charged particles in bacteria inactivation by plasma of a positive and negative corona in ambient air, Plasma Process. Polym. 11(4) (2014) 315–334.

12. **Koval'ová Z., Tarabová K., Hensel K., Machala Z.,** Decontamination of *Streptococci* biofilms and *Bacillus cereus* spores on plastic surfaces with DC and pulsed corona discharges, Europ. Phys. J. – Appl. Phys. 61 (2) (2013) 24306.

13. **Akishev Y. S., Dem'yanov A. V., Karal'nik V. B., et al.,** Comparison of the AC barrier corona with DC positive and negative coronas and barrier discharge, Plasma Phys. Rep. 29 (1) (2003) 82–91.

14. **Timoshkin I. V., Maclean M., Wilson M. P., et al.,** Bactericidal effect of corona discharges in atmospheric air, IEEE Trans. Plasma Sci. 40 (10) (2012) 2322–2333.

15. **Koutsoubi J. M., MacGregor J.,** Electrode erosion and lifetime performance of a high repetition rate, triggered, corona-stabilized switch in air, J. Phys. D. Appl. Phys. 33 (9) (2000) 1093–1103.

16. **Eichwald O., Ducasse O., Dubois D., et al.,** Experimental analysis and modelling of positive streamer in air: towards an estimation of O and N radical production, J. Phys. D. Appl. Phys. 41 (23) (2008) 234002.

17. **Komuro A., Ono R.,** Two-dimensional simulation of fast gas heating in an atmospheric pressure streamer discharge and humidity effects, J. Phys. D. Appl. Phys. 47 (15) (2014) 155202.

18. **Luque A., Ratushnaya V., Ebert U.,** Positive and negative streamers in ambient air: modelling evolution and velocities, J. Phys. D. Appl. Phys. 41 (23) (2008) 234005.

19. **Šimek M.,** Optical diagnostics of streamer discharges in atmospheric gases, J. Phys. D. Appl. Phys. 47(46) (2014) 463001.

20. **Townsend J. S., Edmunds P. J.,** The discharge of electricity from cylinders and points, Philos. Mag. Ser. 6. 27 (161) (1914) 789–801.

21. **Henson B. L.,** A space-charge region model for microscopic steady coronas from points, J. Appl. Phys. 52 (2) (1981) 709–715.

СПИСОК ЛИТЕРАТУРЫ

1. **Fridman A., Friedman G.** Plasma medicine. Chichester, UK: John Wiley & Sons Limited, 2013. 560 p.

2. **Kong M. G., Kroesen G., Morfill G., Nosenko T., Shimizu T., van Dijk J., Zimmermann J. L.** Plasma medicine: an introductory review // New Journal of Physics. 2009. Vol. 11. No. 11. P. 115012.

3. **Dobrynin D., Fridman G., Friedman G., Fridman A.** Physical and biological mechanisms of direct plasma interaction with living tissue // New Journal of Physics. 2009. Vol. 11. No. 11. P. 115020.

4. **Dubois D., Merbahi N., Eichwald O., Yousfi M., Benhenni M.** Electrical analysis of positive corona discharge in air and N_2, O_2, and CO_2 mixtures // Journal of Applied Physics. 2007. Vol. 101. No. 5. P. 053304.

5. **Sekimoto K., Gonda R., Takayama M.** Effects of H_3O^+, OH^-, O_2^-, NO_x^- and NO_x for *Escherichia coli* inactivation in atmospheric pressure DC corona discharges // Journal of Physics D: Applied Physics. 2015. Vol. 48. No. 30. P. 305401.

6. **Weltmann K. D., von Woedtke T**. Plasma medicine – current state of research and medical application // Plasma Physics and Controlled Fusion. 2016. Vol. 59. No. 1. P. 014031.

7. **Moreau E., Audier P., Benard N.** Ionic wind produced by positive and negative corona discharges in air // Journal of Electrostatics. 2018. Vol. 93. June. Pp. 85—96.

8. Райзер **Ю. П.** Физика газового разряда. 3-е изд., перераб. и доп. Долгопрудный: Интеллект, 2009. 736 с.

9. **Castle G. P., Inculet I. I., Burgess K. I.** Ozone generation in positive corona electrostatic precipitators // IEEE Transactions on Industry and General Applications. 1969. Vol. IGA-5. No. 4. Pp. 489—496.

10. **Giacometti J. A., Oliveira O. N.** Corona charging of polymers // IEEE Transactions on Electrical Insulation. 1992. Vol. 27. No. 5. Pp. 924—943.

11. **Sysolyatina E., Mukhachev A., Yurova M., Grushin M., Karalnik V., Petryakov A., Trushkin N., Ermolaeva S., Akishev Y.** Role of the charged particles in bacteria inactivation by plasma of a positive and negative corona in ambient air // Plasma Processes and Polymers. 2014. Vol. 11. No. 4. Pp. 315—334.

12. **Koval'овб Z., Tarabovб K., Hensel K., Machala Z.** Decontamination of *Streptococci* biofilms and *Bacillus cereus* spores on plastic surfaces with DC and pulsed corona discharges // The European Physical Journal — Applied Physics. 2013. Vol. 61. No. 2. P. 24306.

13. **Akishev Y. S., Dem'yanov A. V., Karal'nik V. B., Monich A. E., Trushkin N. I.** Comparison of the AC barrier corona with DC positive and negative coronas and barrier discharge // Plasma Physics Reports. 2003. Vol. 29. No. 1. Pp. 82—91.

14. **Timoshkin I. V., Maclean M., Wilson M. P., Given M. J., MacGregor S. J., Wang T., Anderson J. G.** Bactericidal effect of corona discharges in atmospheric air // IEEE Transactions on Plasma Science. 2012. Vol. 40. No. 10. Pp. 2322—2333.

15. **Koutsoubi J. M., MacGregor J.** Electrode erosion and lifetime performance of a high repetition rate, triggered, corona-stabilized switch in air // Journal of Physics D: Applied Physics. 2000. Vol. 33. No. 9. Pp. 1093—1103.

16. **Eichwald O., Ducasse O., Dubois D., Abahazem A., Merbahi N., Benhenni M., Yousfi M.** Experimental analysis and modelling of positive streamer in air: towards an estimation of O and N radical production // Journal of Physics D: Applied Physics. 2008. Vol. 41 No. 23. P. 234002.

17. **Komuro A., Ono R.** Two-dimensional simulation of fast gas heating in an atmospheric pressure streamer discharge and humidity effects // Journal of Physics D: Applied Physics. 2014. Vol. 47. No. 15. P. 155202.

18. **Luque A., Ratushnaya V., Ebert U.** Positive and negative streamers in ambient air: modelling evolution and velocities //Journal of Physics D: Applied Physics. 2008. Vol. 41. No. 23. P. 234005.

19. Љimek **M.** Optical diagnostics of streamer discharges in atmospheric gases // Journal of Physics D: Applied Physics. 2014. Vol. 47. No. 46. P. 463001.

20. **Townsend J. S., Edmunds P. J.** The discharge of electricity from cylinders and points // Philosophical Magazine. 1914. Ser. 6. Vol. 27. No. 161. Pp. 789—801.

21. **Henson B. L.** A space-charge region model for microscopic steady coronas from points // Journal of Applied Physics. 1981. Vol. 52. No. 2. Pp. 709—715.

THE AUTHOR

FEKLISTOV Efrem G.
Peter the Great St. Petersburg Polytechnic University
29 Politechnicheskaya St., St. Petersburg, 195251, Russia
efrem.feklistov@mail.ru
ORCID: 0000-0002-7189-6567

СВЕДЕНИЯ ОБ АВТОРЕ

ФЕКЛИСТОВ Ефрем Геннадьевич – *ассистент Высшей школы высоковольтной энергетики Санкт-Петербургского политехнического университета Петра Великого.*
195251, Россия, г. Санкт-Петербург, Политехническая ул., 29
efrem.feklistov@mail.ru
ORCID: 0000-0002-7189-6567

Received 15.06.2021. Approved after reviewing 06.12.2021. Accepted 06.12.2021.
Статья поступила в редакцию 15.06.2021. Одобрена после рецензирования 06.12.2021. Принята 06.12.2021.